

Hunting-based Directional Neighbor Discovery in mmWave Ad Hoc Networks

Yu Wang, Shiwen Mao, *Senior Member, IEEE*, and
Theodore (Ted) S. Rappaport, *Fellow, IEEE*

Abstract—The directional neighbor discovery problem, i.e., *spatial rendezvous*, is a fundamental problem in millimeter wave (mmWave) networks, where directional transmissions are used to overcome the high attenuation. The challenge is how to let the transmitter and receiver beams meet in space under *deafness* caused by directional transmission and reception, where no prior information or coordination is available. In this paper, we present a *Hunting-based Directional Neighbor Discovery* (HDND) scheme for ad hoc mmWave networks, where a node follows a unique sequence to determine its transmission or reception mode, and continuously rotates its directional beam to scan the neighborhood for neighbors. Through a rigorous analysis, we derive the conditions for ensured neighbor discovery, as well as a bound for the worst case discovery time. We validate the analysis with extensive simulations, and demonstrate the superior performance of the proposed scheme over two benchmark schemes.

Keywords—5G Wireless; beamforming; spatial filtering; directional antenna; directional neighbor discovery; initial access; mmWave networks; spatial rendezvous.

I. INTRODUCTION

With booming interest in wireless applications and services, there has been a drastic increase in mobile data in recent years, as observed in several industrial white papers (e.g., Cisco's Visual Network Index Report and Qualcomm's 1000× Mobile Data Challenge), and the trend is expected to continue into the next decade. The predicted 1000 times mobile data increase poses unprecedented challenges to existing and future wireless networks, and triggers huge interest in future 5G wireless systems. To this end, millimeter wave (mmWave) communications has been recognized as a key component of 5G wireless, as the huge amount of spectrum in the mmWave bands can enable multi-Gigabit wireless networks and support bandwidth-intensive applications [1]–[4].

There are many challenges on fully harvesting the high potential of mmWave communications. Particularly, mmWave signals experience much higher attenuation than that in lower

frequencies in the first meter of propagation [5], thus requiring directional antennas to overcome this physical phenomenon. Such signals usually do not easily penetrate or diffract around obstacles [3]. Smart antennas and beamforming are indispensable for overcoming the high attenuation and achieving high data rates [6], [7], [17]. Therefore, although studied in the context of cellular and ad hoc networks, there has been renewed interest in the design of directional networks [8]–[11]. A particular fundamental problem in such networks is how to discover neighbors under *deafness* caused by directional transmission and reception, and other problems include the need to bootstrap directional beamsteering in a mmWave network, and to maintain network connectivity when nodes come and go and as propagation conditions and topology vary over time. Fast algorithms without needing centralized control and synchronized operations, yet with guaranteed neighbor discovery, would be highly appealing and useful.

Neighbor discovery is an important component for distributed, autonomous wireless networks [26]. The employment of directional antennas brings about many benefits, but causes great challenges to neighbor discovery. Most existing neighbor discovery schemes are based on certain channel models. MmWave channels are known to be sparse due to limited number of dominant propagation paths. Comprehensive data, surveys and a tutorial of spatial channel models can be found in [5], [24], [35]. In a recent work [17], compressed sensing based low-complexity algorithms are proposed to exploit channel sparsity for adaptively estimating multipath mmWave channel parameters. In another recent work [18], the authors propose a method for estimation of the receive-side spatial covariance matrix of a channel from a sequence of power measurements made at random angles.

The directional neighbor discovery problem is actually a *spatial rendezvous problem*, where the directional beams of a pair of nodes need to meet in space (i.e., pointing to each other or both viewing a strong reflector), with one node in the transmission mode and the other in the reception mode. Existing neighbor discovery schemes for directional wireless networks exploit several approaches to overcome the deafness problem, which is much more severe in mmWave networks due to the narrow beamwidths, such as using omni-directional transmission/reception for neighbor discovery [10]–[14], synchronized operation [12], [13], [15], adopting a centralized control channel [15], and transmission at random directions and exploiting reflected signals [16]–[19]. In the context of cellular mmWave networks, directional neighbor discovery is also called *initial access*, i.e., the procedure with which a

Manuscript received Apr. 17, 2017; revised Sept. 26, 2017; accepted Nov. 10, 2017. This work was supported in part by the National Science Foundation under Grants CNS-1320664 and CNS-1320472, the NYU WIRELESS Industrial Affiliates program, and by the Wireless Engineering Research and Education Center (WEREC) at Auburn University, Auburn, AL, USA. This work is presented in part at IEEE ICDCS 2017, Atlanta, GA, June 2017.

Y. Wang and S. Mao are with the Dept. of Electrical & Computer Engineering, Auburn University, Auburn, AL 36849-5201, USA. T.S. Rappaport is with the NYU WIRELESS Center, NYU Tandon School of Engineering, Brooklyn, NY 11201, USA. Email: yzw0049@tigermail.auburn.edu, smao@ieee.org, tsr@nyu.edu.

Copyright©2017 IEEE. Personal use of this material is permitted. However, permission to use this material for any other purposes must be obtained from the IEEE by sending a request to pubs-permissions@ieee.org.

Digital Object Identifier XXXX/YYYYYY

mobile device establishes an initial link layer connection to a base station [19]–[22]. For instance, in [19], the authors present a directional cell discovery procedure where base stations periodically transmit synchronizations signals at random directions, and the mobiles scan for such signals to detect the base station. In [23], a deterministic approach is proposed with bounded discovery time, by using the Chinese Remainder Theorem on a sector based directional network [25].

A. Related Work

Existing directional neighbor discovery algorithms can be roughly classified as follows.

a) Algorithms Using Other Spectrum Bands: In [15], a multi-band directional neighbor discovery scheme is presented, which uses a common control channel on the 2.4 GHz WiFi band to identify all potential neighbors. This is a centralized scheme that schedules neighbor discovery for the 60 GHz WiFi band. The use of WiFi bands greatly simplifies the process, since all nodes are within one hop in the 2.4 GHz WiFi band, although they do not see each other in the 60 GHz WiFi band.

b) Algorithms Using Omni-directional Communications: In [13], the authors present a synchronized slotted scheme that uses a directional antenna at the transmitter to enhance the gain, and an omni-directional antenna at the receiver to increase the reception probability. A similar approach is adopted in [30] for neighbor discovery in 60 GHz Wireless Personal Area Networks. An angle of arrival (AOA) based algorithm is used to determine the transmitter location. The authors in [12] present a synchronized slotted algorithm that uses the antenna without beamforming (N-BF), transmitter beamforming only (T-BF), and transmitter and receiver beamforming (TR-BF) at different stages of neighbor discovery with a pure randomized algorithm. In these works, the use of omni-directional communications helps to mitigate the deafness problem in directional wireless networks. In [31], the authors present the Talk More Listen Less (TMLL) design principle to reduce idle-listening in neighbor discovery protocols. This work is more suitable for wireless sensor networks where energy consumption is a major concern and transmissions are broadcast based.

c) Algorithms with Synchronized Operation: The above schemes requires synchronized slotted time [12], [13], [15], [30]. Some other schemes have stronger assumptions on synchronized operation [32], [33], such as that all transmitters face a certain direction, all receivers face the opposite direction simultaneously, and all nodes rotate at the same angular velocity. The strongly synchronized operations may lead to more collisions. In [32], a three-way handshake and a random response scheme are used to reduce the collision probability. In [33], a token based algorithm ensures that only one node transmits beacon signals at a time.

d) Randomized Asynchronous Algorithms: Randomized asynchronous algorithms have been developed in [13], [18], [19], [34]. It is shown that asynchronous algorithms require at least twice as much time than a synchronized algorithm for a K -clique network [13], while the performance of the asyn-

chronous algorithm is worse than the synchronized algorithm in general one-way handshake networks [34].

e) Deterministic Algorithms: In [33], the neighbor discovery process is carried out by the nodes sequentially (i.e., serialized), and the scheme discovers all sector-to-sector links between nodes with a systematic approach. In [23], all sector directional pairs are examined with the Chinese Remainder Theorem. A bounded time-distributed neighbor discovery is achieved under the assumption of ideal beacons (i.e., it takes zero time to transmit and receive).

B. Contributions and Organization

In this paper, we consider a mmWave ad hoc network deployed on a 2D area, and develop an effective scheme for neighboring nodes (or, users) to discover each other. Since neighbor discovery is the first step to start a self-configuring wireless network, it may not be easy to acquire prior information for centralized coordination, synchronization, or acquiring a common control channel. On the other hand, while making the receiver work in the omnidirectional mode (at a lower rate) can help to mitigate the blindness problem, the omnidirectional receiver may receive beacons from multiple neighbors simultaneously and at smaller SNR per received signal, leading to interference (i.e., more collisions) and requiring more processing to decode the different beacons in a dense network. Unlike prior approaches, here we develop an effective directional neighbor discovery scheme without using omni-directional transmissions, without needing a centralized control channel, and without needing time synchronization and synchronized operation, yet with guaranteed neighbor discovery performance. In other words, we are interested in “blind” neighbor discovery with only directional antennas. As shown below, this approach offers promise for low power sensor networks, and mobile or fixed mmWave networks that seek to maximize SNR through narrowbeam antenna implementation whenever possible.

In our proposed scheme, a node continuously rotates its directional beam in either the clockwise or counterclockwise direction in a 2D plane, to scan its neighborhood to discover neighbors in a quasi-static mmWave network.¹ While this work focuses on 2D, it should be clear that the method described here could be extended to 3D discovery, for use in networks involving users that have a wide variation in relative elevation, such as drones or for mobile networks for users in high rise buildings. Each node operates either in the *transmission mode* or the *reception mode*. In the transmission mode, the node sends out a beacon signal, stops, and starts to listen for acknowledgments (ACK) from neighbors. The node repeats the beacon-listen pattern when it scans the neighborhood. In the reception mode, the node keeps listening for beacons. If a beacon is received, it responds with an ACK immediately on the same channel. Once a beacon-ACK handshake is completed, the two nodes find each other.

We call this approach *Hunting-based Directional Neighbor Discovery* (HDND), since each node continuously scans its

¹We focus on the 2D network case in this paper, and will extend this approach to 3D networks in our future work using 3D channel models [24].

neighborhood to “hunt” for neighbors (during the neighbor discovery period). Consider a pair of neighboring nodes, where the node with a faster angular velocity for rotating its antenna beam will chase and catch up with the slower node in bounded time. Following the notation in [26], this is a “deterministic” approach, as opposed to random or probabilistic schemes that point to random directions to find neighboring nodes.

Specifically, with the proposed scheme, each node generates its *pseudo-slot sequence* consisting of its ID, a sequence of 0 bits, and a sequence of 1 bits. Each bit corresponds to a pseudo-slot of time. In each pseudo-slot, each node determines its state by the corresponding sequence bit value: transmission mode if it is a 0, and reception mode if it is a 1. A transmitter scans its neighborhood by rotating its beam with angle velocity ω_T . During the scanning process, the transmitter sends a beacon and then starts to listen for ACKs. It repeats the beacon-listen operation, until an ACK is received (i.e., a neighbor is discovered). A receiver also rotates its beam with angle velocity ω_R , while continuously listening for beacons. If a beacon is received, the receiver will reply immediately with an ACK, which completes a successful handshake and the nodes discover each other.

We first consider the basic case of a single transmitter-receiver pair. We derive the condition for the transmitter and receiver beams to meet in the 2D space, derive the distribution of the overlap angle of the two beams, as well as the condition for a successful beacon-ACK handshake (which indicates a successful neighbor discovery). The analysis also sheds useful insights on how to set the protocol parameters to ensure a successful neighbor discovery. We then examine the case of a distributed ad hoc network with randomly placed nodes. We adopt a special sequence design presented in prior work [23], [27], to coordinate the transmission/reception mode of every node without centralized control. We show that when combined with the basic case design of a single transmitter-receiver pair, the proposed scheme can ensure neighbor discovery with bounded discovery time. We derive the procedure for ensured discovery, as well as a bound on the worst case discovery time, and validate our analysis with extensive simulations. By comparing with two benchmark schemes, the proposed algorithm is shown to achieve considerable reduction in neighbor discovery time and substantial gains on network-wide throughput.

The remainder of this paper is organized as follows. Section II presents the system model. Section III examines the case of a transmitter-receiver pair. The proposed scheme is presented in Section IV and validated in Section V. Section VI concludes this paper and discusses future work.

II. SYSTEM MODEL

We consider a mmWave ad hoc network with a set of nodes deployed within an area. We first present the system model and our basic assumptions in the following.

Unique ID: Each node has a unique ID, which is assigned and/or known before the node joins the network.

Steerable Smart Antenna: Each node is equipped with a smart antenna [6], which can continuously steer its beam towards a desired direction [7], [17], e.g., to scan its neighborhood.

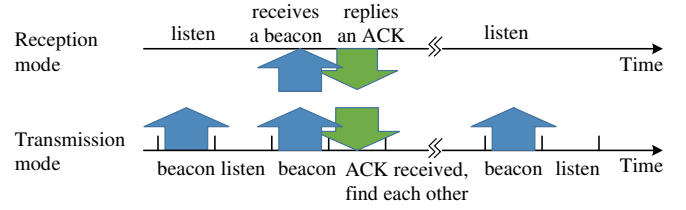


Fig. 1. Example of the transmission and reception modes. The time slot in the figure has a duration of a beacon duration τ_B (plus certain guard time for propagation delay). The first beacon signal is not received since the two beams are not pointing to each other. The second beacon signal is received, and the receiver responds with an ACK, which completes the neighbor discovery procedure.

Beamwidth: The beamwidth of a transmitter, denoted as θ_T , and that of a receiver, θ_R , are constants during the neighbor discovery process, with $0 < \theta_T < 2\pi$ and $0 < \theta_R < 2\pi$.

Antenna Pattern: The antenna pattern for all transceivers is directional (i.e., directional transmitters and directional receivers). The quasi-omnidirectional pattern is not considered since it is inefficient from a link SNR perspective, and not practical for reliable mmWave networks [2], [28]. The pattern for a directional antenna usually consists of a main lobe and several sidelobes. To simplify the model, we ignore the sidelobes and assume that the antenna has an ideal gain as in prior works [29].² Letting ϕ be the pointing angle, which may be within the deviation angle from the center (boresight) of the beam, the antenna gain is modeled as

$$g(\phi) = \begin{cases} G(\theta), & |\phi| < \theta/2 \\ 0, & \text{otherwise.} \end{cases} \quad (1)$$

Communication Mode: We assume the general case of half-duplex nodes. Once turned on, each node operates in one of the two modes, i.e., the *transmission mode* or the *reception mode*. In the transmission mode, a node first sends a short discovery beacon, and then listens for a short period of time for ACK from a discovered neighbor. It repeats the send-listen operation while scanning its neighborhood. In the reception mode, a node continuously listens on the channel while scanning its neighborhood. If a beacon is received, it immediately returns an ACK to the sender of the beacon on the same channel. An example of the communication modes is given in Fig. 1.

Steering Model: Each node can continuously rotate its beam at a constant angular velocity ω_T in the transmission mode and at a different, constant angular velocity ω_R in the reception mode, with the constraint that $\omega_T \neq \omega_R$.³ The same beamwidth, i.e., θ_T and θ_R , and the same antenna gain, i.e., $G(\theta_T)$ and $G(\theta_R)$, are maintained for all the transmitters and receivers, respectively. The angular velocities should satisfy the following constraint:

$$\frac{\omega_R}{\omega_T} = \frac{p}{q}, \quad \text{s.t. } p, q \in \mathbb{Z}^+, p \neq q, \text{ and } \gcd(p, q) = 1, \quad (2)$$

²Sidelobes may be helpful to neighbor discovery, but may also cause more collisions of beacons and ACKs. Attenuated sidelobes will generally be weaker than the main beam. The RX could keep track of relative signal levels to determine the best beam.

³All the nodes use the same ω_T in the transmission mode and the same ω_R in the reception mode. This is pre-configured in the protocol implementation, and of course could be varied as a function of application or node or channel variations.

where $\gcd(\cdot, \cdot)$ returns the greatest common divisor; p and q are different, co-prime, positive integers. If the condition is not satisfied, e.g., $\omega_R = \omega_T$, the two nodes may never find each other.

Discovery Beacon: Each node in the transmission mode continuously sends discovery beacons, containing the transmitter's *Unique ID*. The transmission time of a discovery beacon, i.e., the *beacon duration*, is a short, constant duration τ_B . Without loss of generality, we assume the ACK has a similar format as a beacon, and the transmission time for an ACK is also τ_B .

Successful Discovery A successful neighbor discovery for a pair of nodes i and j , is achieved if node i receives the ID of node j in a beacon and then node i responds with an ACK that carries its ID, or vice versa.

III. NEIGHBOR DISCOVERY FOR A SINGLE TRANSMITTER-RECEIVER PAIR

For ease of exposition, we first examine the fundamental case of a pair of mmWave nodes, one operating in the transmission mode and the other in the reception mode. The findings in this section will then be leveraged to address the case of a mmWave ad hoc network in Section IV.

A. Conditions for a Successful Discovery

With the model described in Section II, a straightforward approach is to let the transmitter and receiver point their beams at random directions; they will discover each other if their beams meet in space (i.e., spatial rendezvous with partial overlap of the pair of beams). However, such a random approach usually leads to a non-negligible probability of missed detection [16]. To mitigate the worst case performance of probabilistic approaches, a *deterministic* algorithm is considered in this paper.

As described in Section II, each node randomly picks a direction (i.e., clockwise or counterclockwise) to rotate its beam at a fixed angular velocity (i.e., ω_T or ω_R , respectively). During rotation, the node in the transmission mode continuously sends a beacon signal and then waits for ACKs, while the node in the reception mode continuously listens for beacons, until they meet in space and complete a beacon-ACK handshake.

We have the following theorem for the proposed scheme.

Theorem 1. *Consider the transmitter-receiver pair case: the receiver has beamwidth θ_R and angular speed ω_R , and the transmitter has beamwidth θ_T and angular velocity ω_T . The angular velocities satisfy constraint (2). The receiver is guaranteed to receive a signal from the transmitter within p rounds (and the transmitter will rotate for q rounds), if and only if the following constraint is satisfied, regardless of the starting positions of the two beams.*

$$p\theta_T + q\theta_R > 2\pi. \quad (3)$$

Proof: Let us begin with a simple example of $p = 4$, $q = 3$, and $\theta_T = \theta_R = \frac{\pi}{3}$. It can be verified that both (2) and (3) are satisfied. Without loss of generality, the receiver (R) rotate clockwise and the transmitter (T) rotate counterclockwise, as shown in Fig. 2. Let t_i 's be the specific time

instances during the scanning process. The initial positions of the transmitter/receiver beams at t_0 are shown in Fig. 2; the transmitter beam is marked as a solid-lined sector, and the receiver beam is marked in a shade of gray.

The two nodes can communicate with each other when their beams meet in space, more specifically, when the transmitter's signal travels along the line connecting them, TR (i.e., *line of centers* (LoC)), and the reception beam covers the LoC at the same time, as the case at time t_3 in Fig. 2.

In Fig. 2, snapshots of the transmitter/receiver antenna beams at different time instances are shown to explain the "hunting" process. Specifically, t_1 and t_2 are the time instances that the transmitter beam starts to reach and leave the LoC, respectively, during the first round of rotation. During interval $[t_1, t_2]$, the receiver radius RS rotates to a new position RS'. The area it sweeps through during this period is marked as a *striped sector* at time t_2 in Fig. 2. After the transmitter beam rotates for $q = 3$ rounds, while the receiver beam rotates for $p = 4$ rounds, there will be three such striped sectors, as shown at time t_6 in Fig. 2.

The striped sectors are generated when the transmitter beam sweeps through the LoC. It can be seen that $t_2 - t_1 = \theta_T / \omega_T$ and thus the central angle of a striped sector is $\theta_T \cdot \omega_R / \omega_T = \theta_T \cdot p / q = 4\pi / 9$. Therefore, after the transmitter beam rotates for $q = 3$ rounds, there will be 3 such striped sectors, each with central angle $4\pi / 9$. Since the transmitter beam rotates at a constant speed, the striped sectors are evenly distributed in the disk, separated by 3 *blank sectors*, each with central angle $2\pi / 9$ (see time t_6 in Fig. 2).

This simple example can be easily generalized. In the general case, after the transmitter beam rotates for exactly q rounds, there will be q striped sectors and q or zero blank sectors. Each time the transmitter beam sweeps through the LoC, the duration is θ_T / ω_T and the central angle of each striped sector is $\theta_T \cdot \omega_R / \omega_T = \theta_T \cdot p / q$. The central angle for each blank sector is $(2\pi - p\theta_T) / q$, when $p\theta_T \leq 2\pi$; otherwise, if $p\theta_T > 2\pi$, the entire disk will be covered in stripes.

Therefore, the receiver is guaranteed to receive part of the beacon after rotating for p rounds, if and only if the receiver beam overlaps with any of the striped sectors. When there are blank sectors, this fact translates to the following condition:

$$(2\pi - p\theta_T) / q < \theta_R \Rightarrow p\theta_T + q\theta_R > 2\pi. \quad (4)$$

When there are no blank sectors (i.e., when $p\theta_T > 2\pi$), the receiver beam will completely overlap with the striped sector (i.e., the entire disk). Combining these two conditions, we have (3). ■

B. Performance Analysis

Theorem 1 provides the condition that the transmitter and receiver beams meet in space. However, *for a successful neighbor discovery, the overlap of the two beams should be sufficiently large for the beacon-ACK handshake to complete*. Define Θ_m as the maximum angle of the overlap of the transmitter and receiver beams. In this section, we provide an analysis of Θ_m to derive its distribution. The analysis also leads to the condition for a successful neighbor discovery.

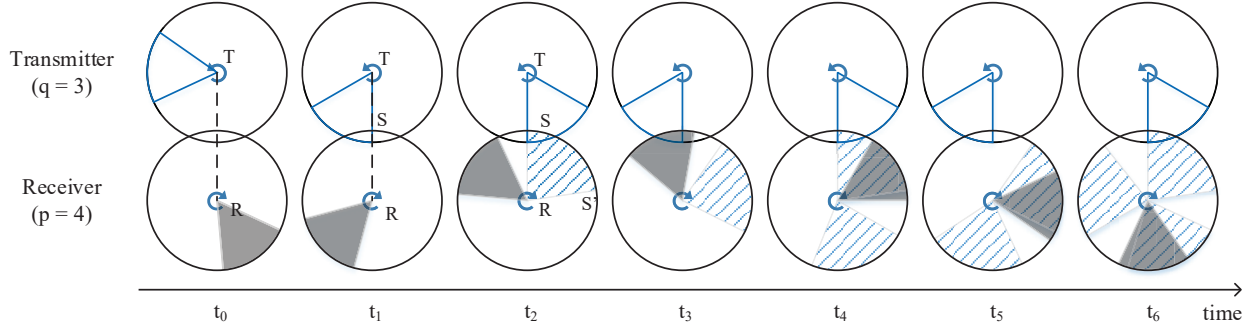


Fig. 2. Relative beam directions of the transmitter and receiver during the neighbor discovery process, during which each beam rotates at a given direction at a constant angular velocity (i.e., ω_T or ω_R). The beam positions of the transmitter and receiver at specific time instances (e.g., t_1, t_2, \dots) are illustrated as a blank sector and a shadow sector, respectively. Note that the time instances are not necessarily evenly spaced. For example, from t_1 to t_2 , the transmitter rotates 60° in the counterclockwise direction, while the receiver rotates 80° in the clockwise direction; from t_2 to t_3 , the transmitter rotates 300° in the counterclockwise direction, while the receiver rotates 400° in the clockwise direction. The ratio is $\omega_T/\omega_R = 60/80 = 300/400 = 3/4$.

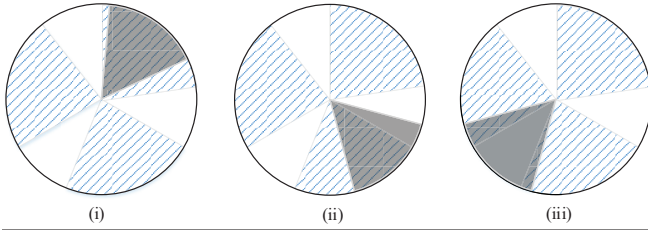


Fig. 3. Three cases for the receiver beam to overlap with the striped sectors. This is the result for the example shown in Fig. 2, after the transmitter beam rotates for $q = 3$ rounds.

Without loss of generality, we assume $p\theta_T > q\theta_R$ in this section (the analysis for the case of $p\theta_T < q\theta_R$ is similar). As shown in the example in Fig. 2, the positions of the striped areas at time t_6 are only dependent on the initial position of the transmitter beam. Then as shown in Fig. 3, if the condition in Theorem 1 is satisfied, there are three possible cases for the transmitter and receiver beams to meet in space:

- 1) The receiver beam is fully covered in a striped sector (as in Fig. 3(i)), due to the assumption $\theta_R < \theta_T \cdot p/q$;
- 2) The receiver beam partially overlaps with *one* striped sector (as in Fig. 3(ii));
- 3) The receiver beam partially overlaps with *two* striped sectors (as in Fig. 3(iii)), since $\theta_R > (2\pi - p\theta_T)/q$ (see Theorem 1).

In Case 1), we have $\Theta_m = \theta_R$ and this happens with probability $(p\theta_T/q - \theta_R)/(2\pi/q) = (p\theta_T - q\theta_R)/(2\pi)$.

In Case 2), part of the receiver beam is covered by a striped area and the other part is covered by a blank area with a central angle of $(2\pi - p\theta_T)/q$. We have $\Theta_m \sim U[(p\theta_T + q\theta_R - 2\pi)/q, \theta_R]$, i.e., Θ_m is uniformly distributed. This happens with probability $2 - p\theta_T/\pi$.

In Case 3), the receiver beam overlaps with two striped sectors; the blank area between the two striped areas is completely covered by the receiver beam. We pick the larger one of the two overlapping areas for Θ_m , which is also uniformly distributed as $U[(p\theta_T + q\theta_R - 2\pi)/(2q), (p\theta_T + q\theta_R - 2\pi)/q]$. This case happens with probability $(p\theta_T + q\theta_R)/(2\pi) - 1$.

Therefore, Θ_m has the following distribution.

$$\Theta_m \sim \begin{cases} \theta_R, & \text{w.p. } \frac{p\theta_T - q\theta_R}{2\pi} \\ U[\frac{p\theta_T + q\theta_R - 2\pi}{q}, \theta_R], & \text{w.p. } 2 - \frac{p\theta_T}{\pi} \\ U[\frac{p\theta_T + q\theta_R - 2\pi}{2q}, \frac{p\theta_T + q\theta_R - 2\pi}{q}], & \text{w.p. } \frac{p\theta_T + q\theta_R}{2\pi} - 1, \end{cases}$$

The probability density function (PDF) of Θ_m is

$$f(\theta_m) = \begin{cases} \frac{p\theta_T - q\theta_R}{2\pi} \cdot \delta(\theta_m - \theta_R), & \text{if } \theta_m = \theta_R \\ \frac{q}{\pi}, & \text{if } \frac{p\theta_T + q\theta_R - 2\pi}{q} < \theta_m < \theta_R \\ \frac{q}{\pi}, & \text{if } \frac{p\theta_T + q\theta_R - 2\pi}{2q} \leq \theta_m \leq \frac{p\theta_T + q\theta_R - 2\pi}{q} \end{cases} \quad (5)$$

where θ_m is the value that r.v. Θ_m takes, and $\delta(\cdot)$ is the Dirac delta function.

The complementary cumulative density function (Complementary CDF) of Θ_m is

$$\bar{F}(\theta_m) = \begin{cases} 0, & \text{if } \theta_m > \theta_R \\ \frac{p\theta_T + q\theta_R - 2q\theta_m}{2\pi}, & \text{if } \frac{p\theta_T + q\theta_R - 2\pi}{2q} \leq \theta_m \leq \theta_R \\ 1, & \text{if } \theta_m < \frac{p\theta_T + q\theta_R - 2\pi}{2q} \end{cases}$$

Define $\tau = 2\tau_B$ as the *handshake time*, i.e., the time required for a successful beacon-ACK handshake. Also let D denote a successful neighbor discovery event. Letting r.v. \mathcal{T} denote the duration when the two beams overlap, the probability for a successful handshake can be derived as

$$P_\tau(D|\mathcal{T} = t) = \begin{cases} 0, & t \leq \tau \\ t/\tau - 1, & \tau < t < 2\tau \\ 1, & t \geq 2\tau \end{cases} \quad (6)$$

Define threshold $\theta_{th} = \tau\omega_R = 2\tau_B\omega_R$. Then the successful handshake probability can be written as

$$P_{\theta_{th}}(D|\Theta_m = \theta_m) = \begin{cases} 0, & \theta_m \leq \theta_{th} \\ \theta_m/\theta_{th} - 1, & \theta_{th} < \theta_m < 2\theta_{th} \\ 1, & \theta_m \geq 2\theta_{th} \end{cases} \quad (7)$$

Theorem 2. Consider the transmitter-receiver pair case. Assuming $p\theta_T + q\theta_R > 2\pi$ and $p\theta_T > q\theta_R$, then for $\theta_{th} = \tau\omega_R$,

the probability for a successful handshake after the transmitter beam rotates for q rounds has the following distribution.

$$P_{\theta_{th}}(D) = \begin{cases} 0, & \text{if } \theta_{th} > \theta_R \\ \frac{q\theta_{th}^2 - q\theta_R\theta_{th} + p\theta_T\theta_R - p\theta_T\theta_{th}}{2\pi\theta_{th}}, & \text{if } \frac{\theta_R}{2} < \theta_{th} \leq \theta_R \\ \frac{p\theta_T + q\theta_R - 3q\theta_{th}}{2\pi}, & \text{if } \frac{p\theta_T + q\theta_R - 2\pi}{2q} < \theta_{th} \leq \frac{\theta_R}{2} \\ \frac{p\theta_T + q\theta_R - \pi - 2q\theta_{th}}{2\pi} - \frac{(p\theta_T + q\theta_R - 2\pi)^2}{8q\theta_{th}\pi}, & \text{if } \frac{p\theta_T + q\theta_R - 2\pi}{4q} < \theta_{th} \leq \frac{p\theta_T + q\theta_R - 2\pi}{2q} \\ 1, & \text{if } \theta_{th} \leq \frac{p\theta_T + q\theta_R - 2\pi}{4q}. \end{cases} \quad (8)$$

Proof: From (7), we have the probability of a successful handshake conditioned on Θ_m . Combining with the distribution of Θ_m given in (5), the probability of having a successful handshake can be derived as

$$\begin{aligned} P_{\theta_{th}}(D) &= \int_0^\infty P_{\theta_{th}}(D|\Theta_m = \theta_m) f(\theta_m) d\theta_m \\ &= \int_{\frac{p\theta_T + q\theta_R - 2\pi}{2q}}^{\theta_R} P_{\theta_{th}}(D|\Theta_m = \theta_m) \frac{q}{\pi} d\theta_m + \\ &\quad \frac{1}{2\pi} (p\theta_T - q\theta_R) P_{\theta_{th}}(D|\theta_R). \end{aligned} \quad (9)$$

The second term in (9) is the integral of the Delta function in (5). Substituting (7) into (9), then we have (8). ■

Theorem 2 indicates that the following corollary holds true, which follows directly by using (8).

Corollary 2.1. *If the chosen parameters satisfy*

$$\tau < (p\theta_T + q\theta_R - 2\pi)/(4q\omega_R), \quad (10)$$

a successful discovery will be guaranteed within q rounds of the transmitter beam rotation.

C. Validation and Discussions

In Figs. 4 and 5, we present simulation results of the transmitter-receiver pair case to validate Theorems 1 and 2. We set both θ_T and θ_R to 30° , and examine the impact of the handshake time τ , rotation parameters p and q , and threshold θ_{th} . The results are obtained from 100,000 simulations with different random seeds.

We find that the simulation results closely match the analysis summarized in Theorem 1 and Theorem 2. Therefore we omit the analysis curves in both figures for clarity. In Fig. 4, we plot the CDF of discovery for increased handshake time, assuming $\theta_{th} = 2^\circ$, to validate Theorem 1. It can be seen that if p and q are small, there is no guarantee of successful discovery over a certain amount of time, since Condition (3) is not satisfied (e.g., when $p = 5$ and $q = 4$, and when $p = 6$ and $q = 5$). When $p = 7$ and $q = 6$, although Condition (3) is satisfied, the overlap of the two beams (i.e., Θ_m) is still too small to guarantee a successful handshake. When p and q are sufficiently large, the CDF curves will reach 100%, as in the case when $p = 11$ and $q = 10$, and when $p = 16$ and $q = 15$.

In Fig. 5, we set $p = 8$ and $q = 7$, which satisfies (3). According to Theorem 2, if θ_{th} is larger than $(p\theta_T + q\theta_R - 2\pi)/(4q)$ (which is 3.2143° in this case), the maximum

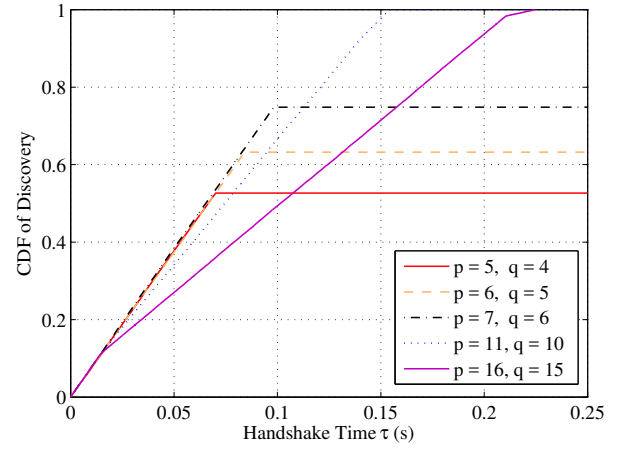


Fig. 4. Cumulative discovery probability versus different p and q values.

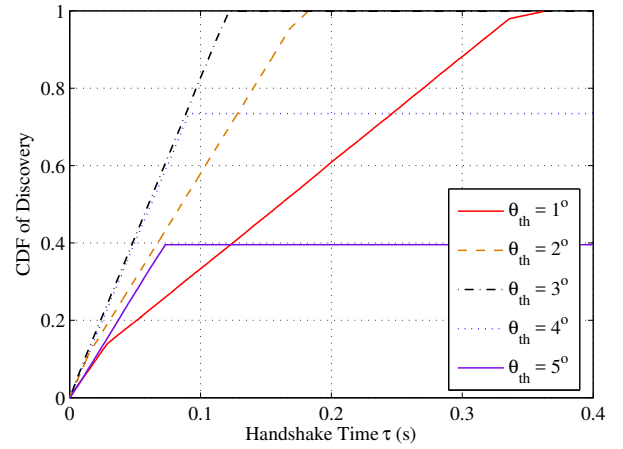


Fig. 5. Cumulative discovery probability versus different θ_{th} values.

probability of discovery should be smaller than 1. That is, successful neighbor discovery may not be guaranteed. For example, see the cases when $\theta_{th} = 4^\circ$ and when $\theta_{th} = 5^\circ$ in Fig. 5, where neighbor discovery may not be ensured since the condition in Theorem 2 is violated. In conclusion, the system parameters θ_R , θ_T , p , q , ω_R , and ω_T must be carefully chosen according to Theorems 1 and 2, to guarantee certain neighbor discovery performance.

IV. HUNTING-BASED DIRECTIONAL NEIGHBOR DISCOVERY

Now, we consider neighbor discovery in a distributed network without centralized control. The key is to make one of the two autonomous neighbors operate in the transmission mode, and the other in the reception mode. We show that this can be achieved with a specific sequence as in prior works [23], [27]. Another issue is the asynchronized operations of the two nodes. Additional discovery time is required when the operations are not aligned. We then derive the worst case bound for neighbor discovery time and present the general neighbor discovery algorithm.

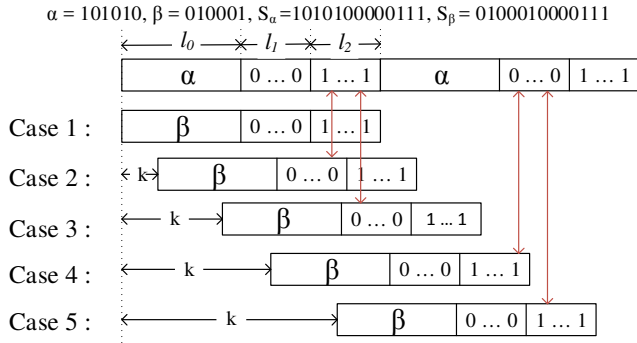


Fig. 6. Example of sequences for mode matching: $\alpha = 101010$, $\beta = 010001$, $l_1 = 4$, and $l_2 = 3$.

A. Mode Matching

Define a *pseudo-slot* as a time slot with a duration of $2\pi q/\omega_T$ (or, $2\pi p/\omega_R$, which is the same due to (2)). That is, the transmitter beam can rotate q rounds, and the receiver beam can rotate p rounds within a pseudo-slot. If a pseudo-slot is marked with “1,” the corresponding node operates in the *transmission mode*; if the pseudo-slot is marked with “0,” the corresponding node operates in the *reception mode* (see the definitions of the transmission and reception modes in Section II). Then we can assign a sequence of 0’s and 1’s to each node, to control the node’s operation mode during the neighbor discovery process without centralized control. If we can guarantee that a node’s “1” pseudo-slot meets the other node’s “0” pseudo-slot at least once within the sequence duration, then according to Theorem 2, these two nodes are guaranteed to find each other.

In [23], [27], a specific control sequence is used to ensure pseudo-slots of different states meet in time for two neighboring nodes. The sequence consists of the node’s unique ID, followed by an l_1 -bit segment of 0’s and an l_2 -bit segment of 1’s. As in the example in Fig. 6, node 1 has ID $\alpha = 101010$ with length $l_0 = 6$, and node 2 has ID $\beta = 010001$ with the same length. Then the sequences for these two nodes are 1010100000111 and 0100010000111 , respectively. Each sequence has length $L = l_0 + l_1 + l_2 = 6 + 4 + 3 = 13$. In [23], [27], it is proven that the two sequences can guarantee at least one bit location with different values, under all possible ways of cyclic rotation within L continuous positions.

Consider different ways of relative cyclic rotations in the general case, while the pseudo-slots of the two nodes are aligned. Using the node 1 sequence as a reference, the node 2 sequence can have a rotation delay k , $k \in [0, L - 1]$. As illustrated in Fig. 6, there are five cases for the relative rotation delay k .

- Case 1: $k = 0$. α is aligned with β . Since both α and β are unique IDs, there is at least one bit location in the first l_0 -bit segment having different values.
- Case 2: $k \in [1, l_2]$. The last bit of the 0-segment in the node 2 sequence is aligned with a bit in the 1-segment in the node 1 sequence.
- Case 3: $k \in [l_2 + 1, l_1 + l_2 - 1]$. The first bit of the 0-segment in the node 2 sequence is aligned with a bit in the 1-segment of the node 1 sequence.

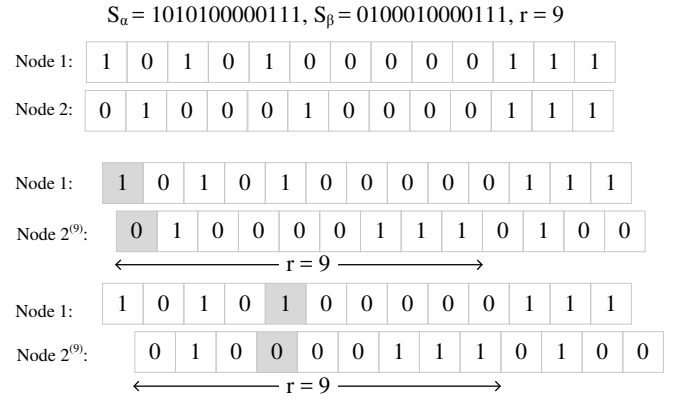


Fig. 7. Finding two pseudo-slots with different states when the pseudo-slots of the two nodes are not aligned (the rotation delay of node β is 9).

- Case 4: $k \in [l_0 + 1, l + l_1 - 1]$. The last bit of the 1-segment in the node 2 sequence is aligned with a bit in the 1-segment in the node 1 sequence.
- Case 5: $k \in [l_0 + l_1, l + l_1 + l_2 - 1]$. The first bit of the 1-segment in the node 2 sequence is aligned with a bit in the 1-segment in the node 1 sequence.

Therefore, the following fact is ensured according to [23], [27].

Fact 1. Using the two sequences, each consists of the node’s unique ID, an l_1 -bit segment of 0’s, and an l_2 -bit segment of 1’s, guarantees that there is at least one pseudo-slot within which the two nodes are in different states during a period of L pseudo-slots, under the condition $l_1 + l_2 \geq l_0$ [23], [27].

Next, we consider the more general case when the pseudo-slots of the two nodes are not aligned. In this case, let the relative rotation of node 2 be between r and $r + 1$, i.e., r slots plus a *drift*, which is shorter than a pseudo-slot. Then, each slot of node 1 will overlap with at least half of the corresponding slot of node 2. For example, in Fig. 7, the relative rotation of the node 2 sequence is 9 pseudo-slots (denote such a node as node $2^{(9)}$). If the drift is smaller than 0.5 pseudo-slot, the node 1 sequence has a different state from that of node $2^{(9)}$ at the first slot. Otherwise, the node 1 sequence has a different state from that of node $2^{(9)}$ at the fifth slot. Thus, we redefine the duration of a pseudo-slot (given at the beginning of Section IV-A) as the time for $2q$ rounds for the transmission mode (which is also the time for $2p$ rounds for the reception mode), i.e., $4\pi q/\omega_T$ (or $4\pi p/\omega_R$). We can guarantee successful neighbor discovery with the above design, when the pseudo-slots of the two nodes are not aligned.

B. Neighbor Discovery Algorithm

Recall that a successful neighbor discovery requires that (i) one node receives the other node’s ID in a beacon, and (ii) it returns its ID in an ACK that is successfully received by the beacon node. In Section IV-A, the sequences adopted ensure that within L pseudo-slots, there will be at least one pseudo-slot for which one node is in the transmission state and the other is in the reception state. The transmitter will repeat the process of sending a beacon and listening for ACK. The receiver will keep listening for beacons and reply an

ACK immediately when a beacon is received. Without loss of generality, the handshake time is $\tau = 2\tau_B$. Therefore, neighbor discovery is ensured, as summarized in the following theorem.

Theorem 3. *If two nodes follow the distributed neighbor discovery procedure given below, then a successful neighbor discovery for the node pair is ensured within L pseudo-slots.*

- 1) Each node generates a pseudo-slot sequence consisting of its unique ID (length l_0), a segment of $\lfloor \frac{l_0}{2} \rfloor + 1$ 0's, and a segment of $\lceil \frac{l_0}{2} \rceil$ 1's.
- 2) In any pseudo-slot, if the state is 1, the node repeats the process of sending a beacon (for τ_B) and waiting for ACK (for another τ_B), and scans its neighborhood for $2q$ rounds. If the state is 0, the node keeps listening for beacons, and scans its neighborhood for $2p$ rounds. If a beacon is received, the node will decode the beacon for the transmitter's ID, and immediately return an ACK that carries its ID.
- 3) Each beacon lasts for $\tau_B = (p\theta_T + q\theta_R - 2\pi)/(8q\omega_R)$.

Proof: From part 1) of Theorem 3, we have $\lfloor \frac{l_0}{2} \rfloor + 1 + \lceil \frac{l_0}{2} \rceil = l_0 + 1 > l$. Then following Fact 1 in Section IV-A, the two nodes are guaranteed to meet in time with different modes for at least half of a pseudo-slot within a period of $L = 2l_0 + 1$ pseudo-slots.

From part 2) of Theorem 3, we know that a half pseudo-slot time is sufficient for the transmitter beam to rotate for q rounds and for the receiver beam to rotate for p rounds.

From part 3) of Theorem 3, we have $2\omega_R\tau_B = (p\theta_T + q\theta_R - 2\pi)/(4q)$. Following Theorem 2, a discovery is ensured within q rounds of transmitter beam rotation. ■

The detailed neighbor discovery algorithm is presented in Algorithm 1. Line 1 in Algorithm 1 generates the pseudo-slot sequence to determine the operation mode of the node. Line 4 in Algorithm 1 reads the state of the current pseudo-slot from the sequence. If the state is 1, the node will operate as a transmitter, and execute Lines 5 – 10 to hunt for a neighbor that is in the reception mode. Otherwise, the node operates as a receiver. It keeps listening for beacons; when a beacon is received, it returns an ACK to the sender (see Fig. 1). Note that the algorithm is not terminated after discovering a neighbor. The algorithm will continue to find other neighbors, if any others can be found. From Theorem 3, any pair of nodes should finish neighbor discovery within L pseudo-slots. The algorithm terminates after L pseudo-slots, when all the potential neighbors are found.

Algorithm 1 is focused on neighbor discovery only. Alternatively, we can leverage the neighbor discovery algorithm for transmission scheduling: when a neighbor is discovered, the transmitter can send a data packet if needed. The motivations for integrating neighbor discovery with transmission scheduling are: (i) after each node discovers its neighbors, a scheduling algorithm will be executed anyway for packet transmissions; (ii) the position and orientation of a node may vary over time, and thus it is beneficial to immediately transmit a backlogged packet when the target neighbor is discovered.

The detailed algorithm for combining neighbor discovery and scheduling is given in Algorithm 2. Once a neighbor is

Algorithm 1: Hunting-based Directional Neighbor Discovery Algorithm

```

1 Each node generates its pseudo-slot sequence  $S$  consisting of
  its ID ( $l_0$  bits),  $\lfloor \frac{l_0}{2} \rfloor + 1$  "0" bits and  $\lceil \frac{l_0}{2} \rceil$  "1" bits;
2  $i \leftarrow 0$ ;
3 if  $i < L$  then
4   if  $S(i) = 1$  then
5     Continuously sends a beacon and listens for ACK
       alternatively for  $2q$  rounds with angle velocity  $\omega_T$ ;
6     if An ACK is received during  $2q$  rounds then
7       A neighbor is discovered;
8       Continue sending and listening for other neighbors;
9     else
10       $i++$ ;
11      Go to Step 3;
12    end
13  else
14    Keep listening for  $2p$  rounds with angle velocity  $\omega_R$ ;
15    if A beacon is received during  $2p$  rounds then
16      Reply an ACK immediately;
17    else
18       $i++$ ;
19      Go to Step 3;
20    end
21  end
22 else
23   Terminate;
24 end

```

discovered, a data packet is transmitted/exchanged between the two nodes, assuming greedy sources (i.e., that there is always data to be transmitted for any other node in the network). Such an approach is particularly useful when the network topology is dynamic (e.g., with mobility). We evaluate the throughput performance of this algorithm in Section V.

C. Worst Case Neighbor Discovery Time

Theorem 3 shows that neighbor discovery can be finished in bounded time, i.e., L pseudo-slots, which is an upper bound on the neighbor discovery time. To further reveal the performance of the proposed scheme, we derive the time needed to discover all neighbors, termed *worst case discovery time* in number of beacon durations (i.e., τ_B), and denoted as N_B , based on all possible initial beam directions, sequences rotations, and sequence drifts. According to the procedure described in Algorithm 1, the worst case discovery time can be written as

$$N_B = 2Lp \frac{2\pi}{\omega_R\tau_B} = \frac{32pqL\pi}{p\theta_T + q\theta_R - 2\pi}. \quad (11)$$

Theorem 4. *The lower bound for worst case neighbor discovery time is $64\pi^2 L/(\theta_T\theta_R)$, in number of beacon durations.*

Proof: Consider the worst case neighbor discovery time, which contains N_B beacon durations as given in (11). Taking partial derivative of N_B with respect to p and q to solve for the minimum, we have

$$\frac{\partial N_B}{\partial p} = \frac{32ql\pi(q\theta_R - 2\pi)}{(p\theta_T + q\theta_R - 2\pi)^2}, \quad \frac{\partial N_B}{\partial q} = \frac{32pl\pi(p\theta_T - 2\pi)}{(p\theta_T + q\theta_R - 2\pi)^2}.$$

On one hand, the potential minimal value of N_B , denoted as N_B^* , is at $\{p_0 = 2\pi/\theta_T, q_0 = 2\pi/\theta_R\}$, with $N_B^* =$

Algorithm 2: Hunting-based Directional Neighbor Discovery Algorithm with Transmission Scheduling.

```

1 Each node generates its pseudo-slot sequence  $S$  consisting of
  its ID ( $l_0$  bits),  $\lfloor \frac{l_0}{2} \rfloor + 1$  "0" bits and  $\lceil \frac{l_0}{2} \rceil$  "1" bits;
2  $i \leftarrow 0$ ;
3 if  $i < L$  then
4   if  $S(i) = 1$  then
5     Continuously sends a beacon and listens for ACK
      alternatively for  $2q$  rounds with angle velocity  $\omega_T$ ;
6     if An ACK is received during  $2q$  rounds then
7       A neighbor is discovered;
8       Send a data packet to the discovered neighbor;
9        $i \leftarrow 0$ ;
10      Go to Step 3;
11    else
12       $i++$ ;
13      Go to Step 3;
14    end
15  else
16    Keep listening for  $2p$  rounds with angle velocity  $\omega_R$ ;
17    if A beacon is received during  $2p$  rounds then
18      Reply an ACK immediately;
19      Receive the data packet;
20       $i \leftarrow 0$ ;
21      Go to Step 2;
22    else
23       $i++$ ;
24      Go to Step 3;
25    end
26  end
27 else
28   Reset  $i \leftarrow 0$ ; Go to Step 2;
29 end

```

$(64\pi^2 L)/(\theta_T \theta_R)$. On the other hand, $\frac{\partial^2 N_B}{\partial^2 p} \big|_{p=p_0} > 0$ and the Hessian is greater than 0. Therefore, $N_B^* = \frac{64\pi^2 L}{\theta_T \theta_R}$ is a lower bound for the worst case neighbor discovery time. ■

V. SIMULATION STUDY

In this section, we present our simulation study on validating the proposed hunting-based directional neighbor discovery algorithm (HDND). We implemented Algorithms 1 and 2 in Matlab and conducted extensive simulations. The simulations for the case of one pair of nodes are repeated 200,000 times with different random seeds, random initial delay and drift of sequences, and random original beam orientations. The initial delay is uniformly distributed in $[0, 100,000]$ beacon durations. We choose the beamwidth for the reception mode as 72° , $360^\circ/11 = 32.73^\circ$, and $360^\circ/23 = 15.65^\circ$, and the beamwidth for the transmission mode as 60° , 30° , and 15° as in [13]. The other parameters are varied during simulations to investigate algorithm performance. The *Oblivious Directional Neighbor Discovery Algorithm* (ODND) presented in [23] (where each node follows the directional sequence assigned according to the Chinese Remainder Theorem, such that any pair of nodes will face to any combination of directions) and a *random scheme* (where each node randomly points its beam to arbitrary directions) are used as benchmarks in these simulations.

In Figs. 8, 9, and 10, the neighbor discovery times for different parameter settings are presented. We find HDND

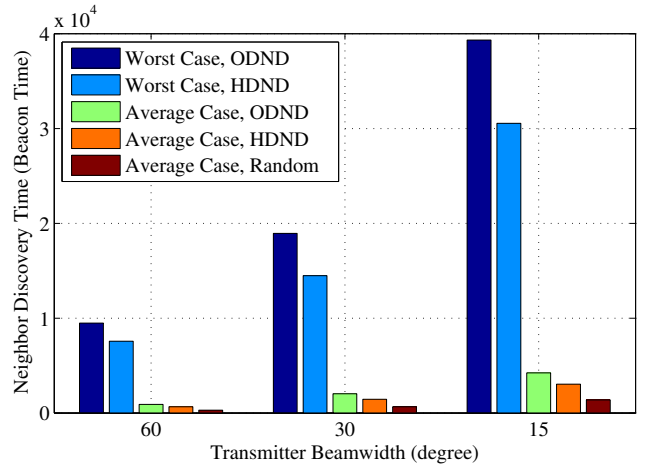


Fig. 8. Neighbor discovery time: receiver beamwidth $\theta_R = 72^\circ$.

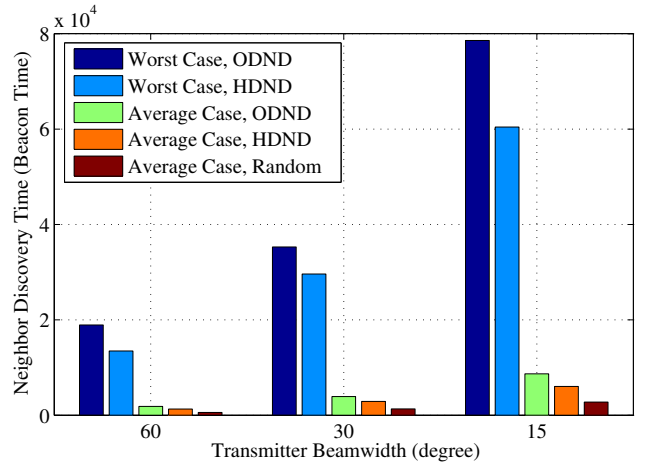


Fig. 9. Neighbor discovery time: receiver beamwidth $\theta_R = 360^\circ/11 = 32.73^\circ$.

outperforms ODND in all the simulations with respect to both worst case and average case discovery times. For example, in Fig. 8, when the transmitter antenna beamwidth is 15° , the worst case discovery time (in number of beacon durations) of ODND is 39330, while that for HDND is 30547, a 22.3% reduction. The average case discovery time of ODND is 4288.6, while that for HDND is 3034, a 29.3% reduction. Although the average case discovery time of Random is the lowest, its worst case discovery time is ∞ (i.e., in many cases it fails to discover the other node), while both HDND and ODND guarantee successful discovery of neighbors. The discovery times (worst case and average case) of all the schemes increase as the antenna beamwidths are reduced, due to the more severe deafness effect caused by highly directional antennas.

To make a fair comparison with ODND, we relax the ideal beacon assumption made for ODND in [23] (i.e., a zero beacon duration), and use real beacons with a non-zero transmission time in the simulations. We set 10 beacons per slots, since the positions of beacons in [23] are at the 10% and 20% positions of a slot. Otherwise, there will be a collision even without considering the drift effect. For Random, a pair of nodes may

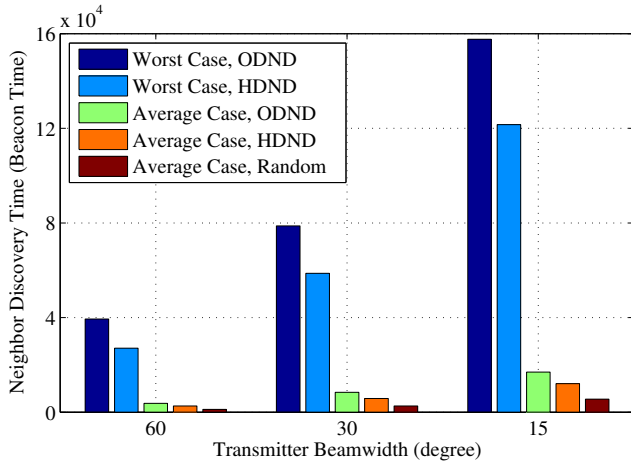


Fig. 10. Neighbor discovery time: receiver beamwidth $\theta_R = 360^\circ/23 = 15.65^\circ$.

not discover each other within 200,000 beacon durations. We also find that ODND may not always discover all neighbors, when removing the ideal beacon assumption. From Figs. 8, 9, and 10, the worst case delay and average delay values show the proposed HDND algorithm has a speed-up ratio between 1.3 to 1.5 times than ODND in both worst case delay and average delay in all tested scenarios.

Simulation results for a distributed mmWave network are given in Figs. 11, 12, and 13, where 100 nodes are randomly placed in a 20.0×20.0 m² square region. The simulation parameters are presented in Table I. The unit time is the beacon duration τ_B . For example, in Fig. 11, a value 5000 means $5000\tau_B$ s. The network topology is randomly generated for each simulation configuration, and we plot 95% confidence intervals for all the curves. From Figs. 11 and 12, we find that Algorithm 1's average and worst case total neighbor discovery time are almost constant as the transmission range is increased from 2.5 m to 12.5 m. ODND average discovery time also remains constant, but the worst case discovery time increases with increased transmissions range. Still, Algorithm 1 is about 1.4 times faster in discovery time than ODND. The missed detection ratio is presented in Fig. 13 for the network simulations. Algorithm 1 presented here can find almost all neighbors following the setting in [23], as Fig. 13 shows that the missed detection rate is almost 0% for all simulated cases. ODND has a 0.4% chance to miss neighbors due to collision of beacons. Note that miss-detection of neighbors in Algorithm 1 is caused by collisions of beacons only. If the same ideal beacon assumption is made (i.e., extremely short beacons zero transmission time for beacons), the miss-detection probability will be zero for HDND.

To evaluate the proposed Algorithm 1 under more realistic scenarios, we next examine the impact of transmission errors (i.e., loss of beacons or ACKs due to bit errors). Clearly, loss of beacons and/or ACKs will reduce the success rate of neighbor discovery, or increase the neighbor discovery time. The impact of errors can be mitigated by adopting a stronger error correction code for beacon transmissions and ACKs sent by the receiving node. We conduct simulations with

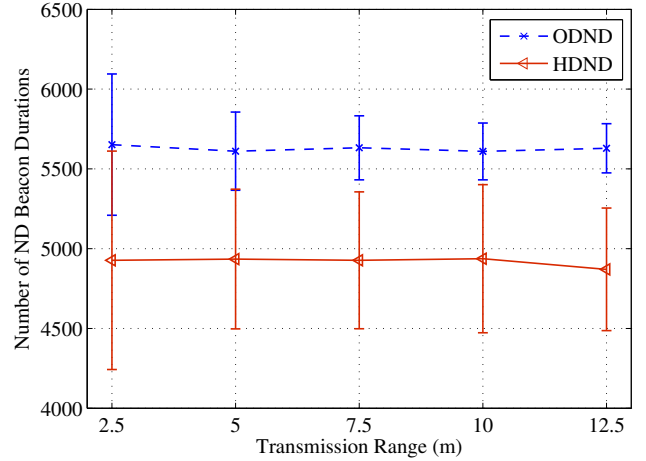


Fig. 11. Average case neighbor discovery time versus transmission range.

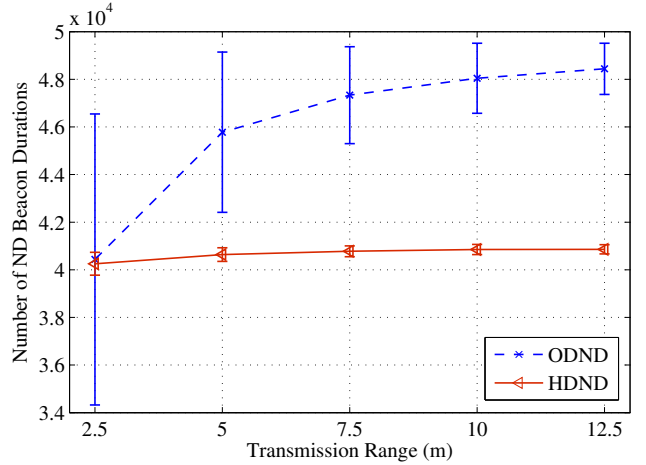


Fig. 12. Worst case neighbor discovery time versus transmission range.

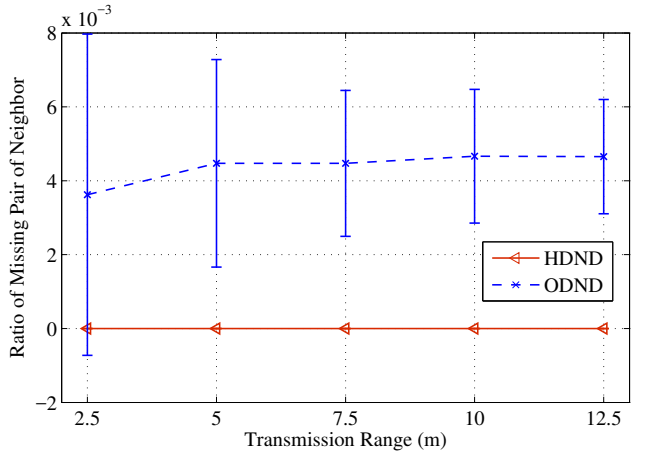


Fig. 13. Miss detection rate versus transmission range.

different packet error rates for beacon/ACK transmissions. The results are presented in Figs. 14 and 15. We find that, not surprisingly, the average and worst neighbor discovery time are both increased as the packet error rate is increased, for both

TABLE I
SIMULATION PARAMETERS

Parameter	Value
Network area	20 m × 20 m
Transmission range	2.5/5.0/7.5/10.0/12.5 m
Number of nodes	10, 20, 30, 40
Directional beamwidth	30°
Control package length	1074 bytes
Data package length	10 Mbytes
Control data rate (mmWave band)	27.5 Mbps
Data transmission rate	2503 Mbps

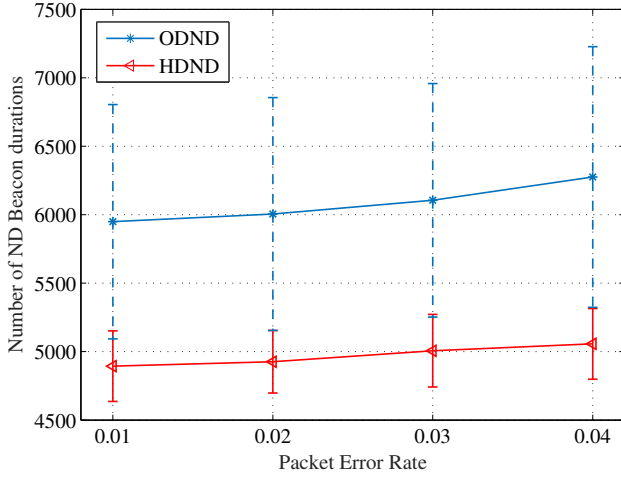


Fig. 14. Average case neighbor discovery time with transmission errors.

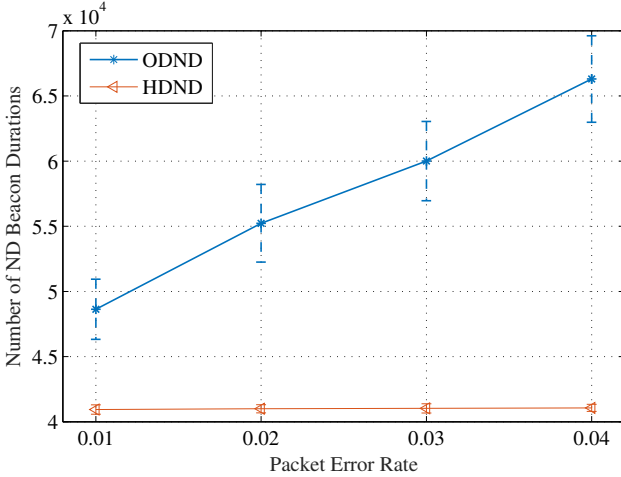


Fig. 15. Worst case neighbor discovery time with transmission errors.

the benchmark scheme and the proposed scheme in Algorithm 1. However, it can be seen that the proposed scheme still outperforms the benchmark scheme with considerable gains. The worst case neighbor discovery time of Algorithm 1 is rather robust to transmission errors. When the packet error rate is increased from 0.01 to 0.04, the worst case neighbor discovery time of HDND is only slightly increased from 40940 to 41063, while worst case neighbor discovery time of ODND is increased from 48632 to 66298.

We also consider the impact of sidelobes. The sidelobe pattern for this simulation consists of a main lobe with a

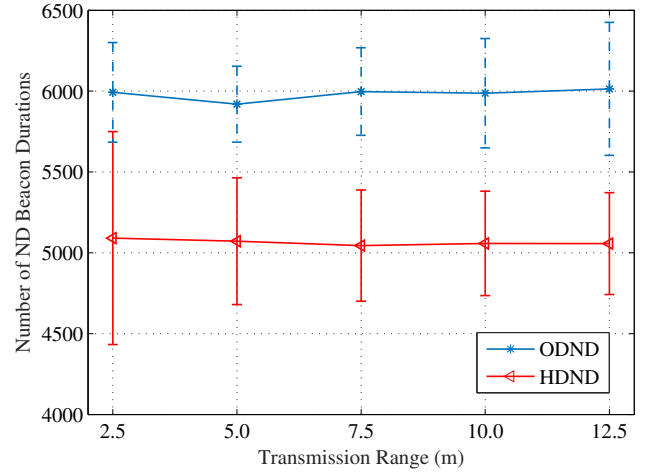


Fig. 16. Average case neighbor discovery time with the sidelobe effect.

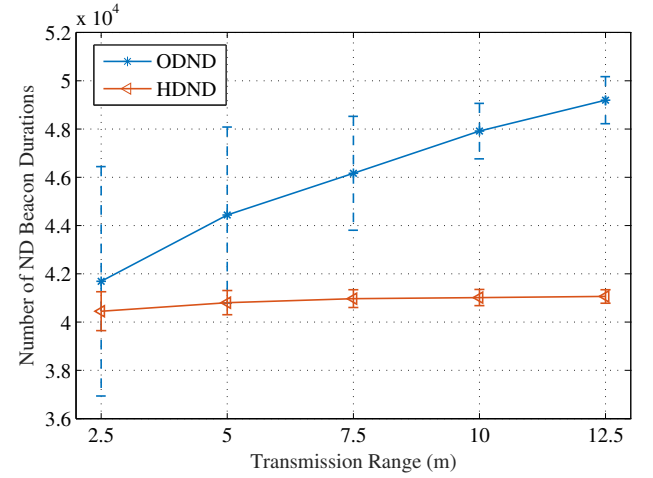


Fig. 17. Worst case neighbor discovery time with the sidelobe effect.

beamwidth of 30°, as well as 8 sidelobes on the remaining directions, each with a beamwidth of 15°. Each of the 8 sidelobes are 6.73 dB down from the main lobe. Similar to the main lobe, a sidelobe can also send or receive beacon signals as well as causing interference/collision to other signals if and only if the sidelobe overlap with other beams [2]. The simulation results are presented in Figs. 16 and 17.

From Figs. 16 and 17, we find that the average neighbor discovery time does not change much with the sidelobe effect, since the sidelobe effect is dependent on the distance between the neighbors. If two nodes are in the transmission range such that they can communicate with each other only with both main lobes, the sidelobes do not affect the neighbor discovery performance. If two nodes are close enough, the sidelobe effect will bring more opportunity of neighbor discovery, as well as collisions. Thus, the sidelobe effect brings about more uncertainty especially when the network is dense. This can be seen in Fig. 17: the worst case neighbor discovery time increases slightly compared to Fig. 12 due to sidelobe uncertainty.

Finally, we evaluate the performance of Algorithm 2. Since HDND achieves significant reductions in neighbor discovery

time than ODN as shown in Figs. 8–17, this would directly translate to higher throughput gain in an actual network. In addition, ODN does not include a transmission scheduling component. Therefore, we consider the Multi-band Neighbor Discovery (MBND) [15] as a benchmark for comparison to Algorithm 2, where all nodes are within a one hop network on the 2.4 GHz WiFi channel, and are coordinated by a central controller.⁴ With MBND, the nodes are scheduled to conduct directional neighbor discovery in the mmWave band, one node pair at a time. The simulation parameters are listed in Table I. Each simulation is repeated 30 times, each time with a randomly generated topology, and 95% confidence intervals are computed and plotted. We consider the greedy source case where a node always has a full buffer of data to send to each neighbor.

The throughput results are presented in Fig. 18 for increasing transmission range. The values of p and q are set according to Theorems 1 and 2, as $p = 13$ and $q = 12$. We find the throughput of Algorithm 2 increases as the number of nodes in the network is increased, as well as the transmission range is increased, while the MBND curves only increase slightly for increased network size and transmission range. The result shows that with the proposed scheme in Algorithm 2, the network capacity can be enhanced as more neighbors are discovered, which allows more concurrent transmissions. The MBND throughput performance is limited by the CSMA/CA mechanism on the 2.4GHz WiFi control channel, which becomes the bottleneck. There are significant gains on throughput achieved by the proposed HDND scheme over MBND, and the gain is greater for larger networks and longer transmission ranges. For example, when the transmission range is 2.5 m and there are 40 nodes in the network, the HDND throughput is 14.31 Gbps and the MBND throughput is 1.96 Gbps, a 7.3 times gain. When the transmission range is 12.5 m for the same network, the HDND throughput is 30.89 Gbps and the MBND throughput is 1.9614 Gbps, a 15.75 times gain.

VI. CONCLUSIONS AND FUTURE WORK

In this paper, we developed a Hunting-based Directional Neighbor Discovery (HDND) scheme for mmWave networks, where nodes rotate their antenna beams to search for neighbors. Based on a rigorous analysis using a deterministic approach, we derived the conditions for guaranteed neighbor discovery as well as a bound for the worst case discovery time. The proposed HDND scheme does not require any control channels, nor does it require any omni-directional transmissions or any synchronized operation or time synchronization. Its performance was validated with simulations. The results indicate remarkable improvement in neighbor discovery time, and striking increases in throughput over a wide range of network topologies compared to prior work.

⁴We chose MBND as a benchmark since it is a recent related work on the topic. Note that the comparison may not be a perfect one, since the design, requirements, and architecture of these two schemes are quite different. Unlike HDND, MBND uses 2.4 GHz WiFi for neighbor discovery and thus the throughput of MBND can be low if the discovery time is considered (or emphasized). However, MBND can provide low discovery time even in mobile environments and dense environments since the discovery procedure can be completed in one shot.

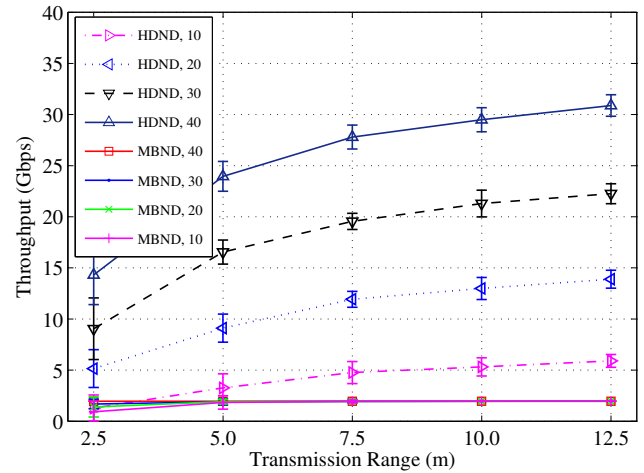


Fig. 18. Network-wide throughput under different transmission ranges.

For future work, a 3D network model will be considered with a more sophisticated directional antenna model. It is also worth investigating how to incorporate a more realistic directional channel model into the protocol design, e.g., the NYUSIM model developed at NYU WIRELESS, while still keeping the problem tractable. It will also be interesting to study the impact of mobility or even the movement of a nearby human (antenna shadowing) on the neighbor discovery performance.

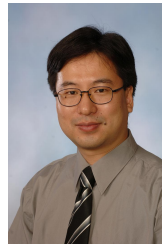
REFERENCES

- [1] Y. Wang, S. Mao, and T.S. Rappaport, "On directional neighbor discovery in mmWave networks," in *Proc. IEEE ICDCS 2017*, Atlanta, GA, June 2017, pp.1–10.
- [2] T.S. Rappaport, R.W. Heath, R.C. Daniels, and J. N. Murdock, *Millimeter Wave Wireless Communications*, Upper Saddle River, NJ: Prentice Hall, 2014.
- [3] T.S. Rappaport, S. Sun, R. Mayzus, H. Zhao, Y. Azar, K. Wang, and F. Gutierrez, "Millimeter wave mobile communications for 5G cellular: It will work!" *IEEE Access J.*, vol.1, pp.335–349, May 2013.
- [4] Z. He and S. Mao, "Adaptive multiple description coding and transmission of uncompressed video over 60GHz networks," *ACM Mobile Comput. Commun. Rev.*, vol.18, no.1, pp.14–24, Jan. 2014.
- [5] S. Sun, T.S. Rappaport, T.A. Thomas, A. Ghosh, H.C. Nguyen, I.Z. Kovacs, I. Rodriguez, O. Koymen, and A. Partyka, "Investigation of prediction accuracy, sensitivity, and parameter stability of large-scale propagation path loss models for 5G wireless communications," *IEEE Trans. Veh. Technol.*, vol.65, no.5, pp.2843–2860, May 2016.
- [6] H.N. Dai, K.W. Ng, M. Li, and M.Y. Wu, "An overview of using directional antennas in wireless networks," *Int. J. Commun. Syst.*, vol.26, no.4, pp.413–448, Apr. 2013.
- [7] T. Ohira and K. Gyoda, "Electronically steerable passive array radiator antennas for low-cost analog adaptive beamforming," in *Proc. IEEE Phased Array 2000*, Dana Point, CA, May 2000, pp.101–104.
- [8] Z. He, S. Mao, and T.S. Rappaport, "On link scheduling under blockage and interference in 60 GHz ad hoc networks," *IEEE Access J.*, vol.3, pp.1437–1449, Sept. 2015.
- [9] Z. He and S. Mao, "A decomposition principle for link and relay selection in dual-hop 60 GHz networks," in *Proc. IEEE INFOCOM 2016*, San Francisco, CA, Apr. 2016, pp.1683–1691.
- [10] I. K. Son, S. Mao, M. X. Gong, and Y. Li, "On frame-based scheduling for directional mmWave WPANs," in *Proc. IEEE INFOCOM 2012*, Orlando, FL, Mar. 2012, pp.2149–2157.
- [11] I.-K. Son, S. Mao, Y. Li, M. Chen, M.X. Gong, and T.S. Rappaport, "Frame-based medium access control for 5G wireless networks," *Springer MONET Journal*, vol.20, no.6, pp.763–772, Dec. 2015.
- [12] R. Ramanathan, J. Redi, C. Santivanez, D. Wiggins, and S. Polit, "Ad hoc networking with directional antennas: A complete system solution," *IEEE Sel. Areas Commun.*, vol.23, no.3, pp.496–506, Mar. 2005.

- [13] S. Vasudevan, J. Kurose, and D. Towsley, "On neighbor discovery in wireless networks with directional antennas," in *Proc. IEEE INFOCOM'05*, Miami, FL, Mar. 2005, pp.2502–2512.
- [14] M. X. Gong, R. J. Stacey, D. Akhmetov, and S. Mao, "A directional CSMA/CA protocol for mmWave wireless PANs," in *Proc. IEEE WCNC 2010*, Sydney, Australia, Apr. 2010, pp.1–6.
- [15] H. Park, Y. Kim, T. Song, and S. Pack, "Multiband directional neighbor discovery in self-organized mmWave ad hoc networks," *IEEE Trans. Veh. Technol.*, vol.64, no.3, pp.1143–1155, Mar. 2015.
- [16] J. Ning, T.S. Kim, S.V. Krishnamurthy, and C. Cordeiro, "Directional neighbor discovery in 60 GHz indoor wireless networks," *Performance Evaluation*, vol.68, no.9, pp.897–915, Sept. 2011.
- [17] S. Sun and T.S. Rappaport, "Millimeter wave MIMO channel estimation based on adaptive compressed sensing," in *Proc. IEEE ICC 2017-Workshops*, Paris, France, May 2017, pp.47–53.
- [18] P.A. Elias, S. Rangan, and T.S. Rappaport, "Low-rank spatial channel estimation for millimeter wave cellular systems," *IEEE Trans. Wireless Commun.*, vol.16, no.5, pp.2748–2759, May 2017.
- [19] C.N. Barati, S.A. Hosseini, S. Rangan, P. Liu, T. Korakis, S.S. Panwar, T.S. Rappaport, "Directional cell discovery in millimeter wave cellular networks," *IEEE Trans. Wireless Commun.*, vol.14, no.12, pp.6664–6678, Dec. 2015.
- [20] C.N. Barati, S.A. Hosseini, M. Mezzavilla, T. Korakis, S.S. Panwar, S. Rangan, & M. Zorzi, "Initial access in millimeter wave cellular systems," *IEEE Trans. on Wireless Commun.*, vol.15, no.12, pp.7926–7940, Sept. 2016.
- [21] W.B. Abbas, M. Zorzi, "Context information based initial cell search for millimeter wave 5G cellular networks," in *IEEE EuCNC 2016*, Athens, Greece, June 2016, pp.111–116.
- [22] Y. Li, J.G. Andrews, F. Baccelli, T.D. Novlan, J.C. Zhang, "Design and analysis of initial access in millimeter wave cellular networks," *IEEE Trans. Wireless Commun.*, vol.16, no.99, pp.1–1, July 2017.
- [23] L. Chen, Y. Li, and A.V. Vasilakos, "Oblivious neighbor discovery for wireless devices with directional antennas," in *Proc. IEEE INFOCOM'16*, San Francisco, CA, Apr. 2016, pp.1–9.
- [24] M.K. Samimi and T.S. Rappaport, "3-D millimeter-wave statistical channel model for 5G wireless system design," *IEEE Trans. Microw. Theory Techn.*, vol.64, no.7, pp.2207–2225, July 2016.
- [25] K. Ireland and M. Rosen, *A Classical Introduction to Modern Number Theory*, 2nd ed., Springer-Verlag, 1990.
- [26] L. Chen and K. Bian, "Neighbor discovery in mobile sensing applications: A comprehensive survey," *Elsevier Ad Hoc Netw.*, vol.48, pp.38–52, Sept. 2016.
- [27] K. Bian and J.-M. J. Park, "Maximizing rendezvous diversity in rendezvous protocols for decentralized cognitive radio networks," *IEEE Trans. Mobile Comput.*, vol.12, no.7, pp.1294–1307, July 2013.
- [28] T. Nitsche, C. Cordeiro, A.B. Flores, E.W. Knightly, E. Perahia, and J.C. Widmer, "IEEE 802.11 ad: Directional 60 GHz communication for multi-Gigabit-per-second Wi-Fi," *IEEE Commun.*, vol.52, no.12, pp.132–141, Dec. 2014.
- [29] R. Mudumbai, S. Singh, and U. Madhow, "Medium access control for 60 GHz outdoor mesh networks with highly directional links," in *Proc. IEEE INFOCOM'09*, Rio de Janeiro, Brazil, Apr. 2009, pp.2871–2875.
- [30] X. An, R.V. Prasad, and I. Niemegeers, "Neighbor discovery in 60 GHz wireless personal area networks," in *Proc. IEEE WoWMoM'10*, Montreal, Canada, June 2010, pp.1–8.
- [31] Y. Qiu, S. Li, X. Xu, and Z. Li, "Talk More Listen Less: Energy-efficient neighbor discovery in wireless sensor networks," in *Proc. IEEE INFOCOM 2016*, San Francisco, CA, Apr. 2016, pp.1–9.
- [32] Z. Zhang, "DTRA: Directional transmission and reception algorithms in WLANs with directional antennas for QoS support," *IEEE Netw.*, vol.19, no.3, pp.27–32, May/June 2005.
- [33] E. Felemban, R. Murawski, E. Ekici, S. Park, K. Lee, J. Park, and Z. Hameed, "SAND: Sectorized-antenna neighbor discovery protocol for wireless networks," in *Proc. IEEE SECON'10*, Boston, MA, June 2010, pp.1–9.
- [34] B. Liu, B. Rong, R. Hu, and Y. Qian, "Neighbor discovery algorithms in directional antenna based synchronous and asynchronous wireless ad hoc networks," *IEEE Wireless Commun.*, vol.20, no.6, pp.106–112, Dec. 2013.
- [35] R.B. Ertrel, P. Cardieri, K.W. Sowerby, T.S. Rappaport, and J.H. Reed, "Overview of spatial channel models for antenna array communication systems," *IEEE Personal Commun.* vol., no., pp.10–22, Feb. 1998.



Yu Wang (S'14) received his B.E. degree in electronic engineering from Tsinghua University, Beijing, China in 2010. He then worked for Weiketong Technology Ltd., Beijing, China, as a technician from 2010 to 2012. He is currently a Ph.D. candidate in the Department of Electrical and Computer Engineering at Auburn University. His research interests include millimeter wave (mmWave) communications and networks, and full-duplex communications.



Shiwen Mao (S'99-M'04-SM'09) received Ph.D. in electrical and computer engineering from Polytechnic University, Brooklyn, NY. Currently, he is the Samuel Ginn Distinguished Professor in the Department of Electrical and Computer Engineering, Auburn University, Auburn, AL. His research interests include wireless networks and multimedia communications. He is a Distinguished Lecturer of the IEEE Vehicular Technology Society. He is on the Editorial Board of IEEE Transactions on Multimedia, IEEE Internet of Things Journal, IEEE Multimedia, ACM GetMobile, among others. He was a past Associate Editor of IEEE Transactions on Wireless Communications and IEEE Communications Surveys and Tutorials. He is the Chair of the IEEE ComSoc Multimedia Communications Technical Committee. He received the 2015 IEEE ComSoc TC-CSR Distinguished Service Award, the 2013 IEEE ComSoc MMTC Outstanding Leadership Award, and the NSF CAREER Award in 2010. He is a co-recipient of the Best Paper Awards from IEEE GLOBECOM 2016, IEEE GLOBECOM 2015, IEEE WCNC 2015, and IEEE ICC 2013, the Best Demo Award from IEEE SECON 2017, and the 2004 IEEE Communications Society Leonard G. Abraham Prize in the Field of Communications Systems.



Theodore (Ted) S. Rappaport (S'83-M'84-SM'91-F'98) received his B.S., M.S., and Ph.D. degrees in electrical engineering from Purdue University, West Lafayette, Indiana, in 1982, 1984, and 1987, respectively. He is an Outstanding Electrical and Computer Engineering Alumnus (OECEA) and Distinguished Engineering Alumnus (DEA) from his alma mater. He holds the David Lee/Ernst Weber Chair in Electrical and Computer Engineering at the New York University (NYU) Polytechnic School of Engineering, and also holds professorships in the Courant computer science department and the NYU medical school (radiology). In 2012, he founded NYU WIRELESS, a multidisciplinary research center involving NYUs engineering, computer science, and medical schools. Earlier in his career, he founded the Wireless Networking and Communications Group (WNCG) at The University of Texas at Austin, and the Mobile and Portable Radio Research Group (MPRG), now known as Wireless@Virginia Tech. He has authored or co-authored more than 200 technical papers, several bestselling technical books, over 100 U.S. and international patents, and cofounded and advised several companies that have contributed to the expansion of the modern wireless communications industry. He was elected to the Board of Governors of the IEEE Communications Society (ComSoc) in 2006, and was elected to the Board of Governors of the IEEE Vehicular Technology Society (VTS) in 2008 and 2011. He served as technical program chairman and program executive for the IEEE GLOBECOM conference in 2004 and 2014, respectively.